P1.11 THE OKLAHOMA MESONET'S SKIN TEMPERATURE NETWORK

Christopher A. Fiebrich*[(1)], Janet E. Martinez[(1)], Jerald A. Brotzge[(2)] and Jeffrey B. Basara[(1)]

[(1)]Oklahoma Climatological Survey, Norman, Oklahoma Climate Survey
[(2)]Center for Analysis and Prediction of Storms,
University of Oklahoma, Norman, Oklahoma

1. INTRODUCTION

Skin temperature (T_s), commonly defined as the temperature of the interface between the Earth's surface and its atmosphere, is a key variable critical to land-atmosphere interactions. For example, T_s is used by Monin-Obukov (1954) similarity theory to estimate sensible heat flux (Kustas et al. 1989; Sugita and Brutsaert 1996; Cahill et al. 1997; Crago 1998; Lhomme et al. 2000; Voogt and Grimmond 2000). Furthermore, T_s is used to estimate latent heat flux (Crago 1998; Ibanez et al. 1999), air temperature and humidity (English 1999), and bare soil evaporation (Katul and Parlange 1992).

In 1999, The Oklahoma Mesonet (Brock et al. 1995), an automated network of 115 meteorological stations evenly spaced across the state (Fig. 1), installed infrared temperature (IRT) sensors at 89 sites. In addition, these Mesonet sites also measure solar radiation, net radiation, air pressure, precipitation, wind speed and direction at 10 m, wind speed at 2 m and 9 m, temperature and relative humidity at 1.5 m, temperature at 9 m, and bare soil and sod temperatures at 5, 10 and 30 cm depths, and soil moisture at several depths. Furthermore, 10 sites that have IRT sensors installed are also designated as OASIS Super Sites (Fig. 1; Brotzge et al. 1999). These sites are equipped to measure incoming and outgoing shortwave and longwave radiation explicitly. The 10 Super Sites estimate sensible and latent heat flux (using an eddy covariance technique) and ground heat flux.

This manuscript provides a description of the IRT sensor, an evaluation of its performance, and selected case studies that display the utility of the sensor and in situ observations of Ts.

*Corresponding author address: Oklahoma Climatological Survey, 100 E. Boyd St., Suite 1210, Norman, OK 73019. Email: chris@mesonet.org

2. DESCRIPTION OF THE IRT SENSOR

2.1. *Sensor installation and calibration equation*

The infrared thermometer used by the Oklahoma Mesonet is a precision thermocouple IRT manufactured by Apogee Instruments, Inc. (Bugbee et al. 1998). This sensor was chosen for use in the network because it was water resistant, specifically designed for continuous outdoor use, and compatible with current Mesonet data acquisition systems. Sensor accuracy is approximately +/- 0.2 °C from 15 to 35 °C and +/- 0.3 °C from 5 to 45 °C. The sensor is installed at a height of 1.5 m and has a 3:1 field of view (i.e., a diameter circle field of view of 0.5 m).

Infrared thermometers estimate skin temperature by measuring a specific waveband within the infrared range, typically 8 to 14 microns (Bugbee et al. 1998). The energy detected by the sensor is converted to a temperature using the Stefan-Boltzman Law and an assumed surface emissivity. Slight error is caused by assuming a surface emissivity; that error is proportional to the difference between the skin and air temperatures (Bugbee et al. 1998).

The final (or calibrated) skin temperature (T_{sc}) is calculated as a function of the difference between the temperatures of the target (land-atmosphere interface) and sensor body. Errors can occur in measuring the sensor body temperature, which then result in errors in T_{sc}. To minimize such errors, a large thermal mass surrounds the reference thermistor to help maintain a more constant sensor body temperature during rapidly changing atmospheric conditions (Bugbee et al. 1998). To account for errors introduced by variations in emissivity and the sensor body temperature, a correction has been provided by Apogee and is applied to all observations. The correction is as follows:

$$T_{sc} = T_{target} - \frac{0.25}{P_{sb}} * \left[\left(T_{target} - H_{sb} \right)^2 - K_{sb} \right] \quad (1)$$

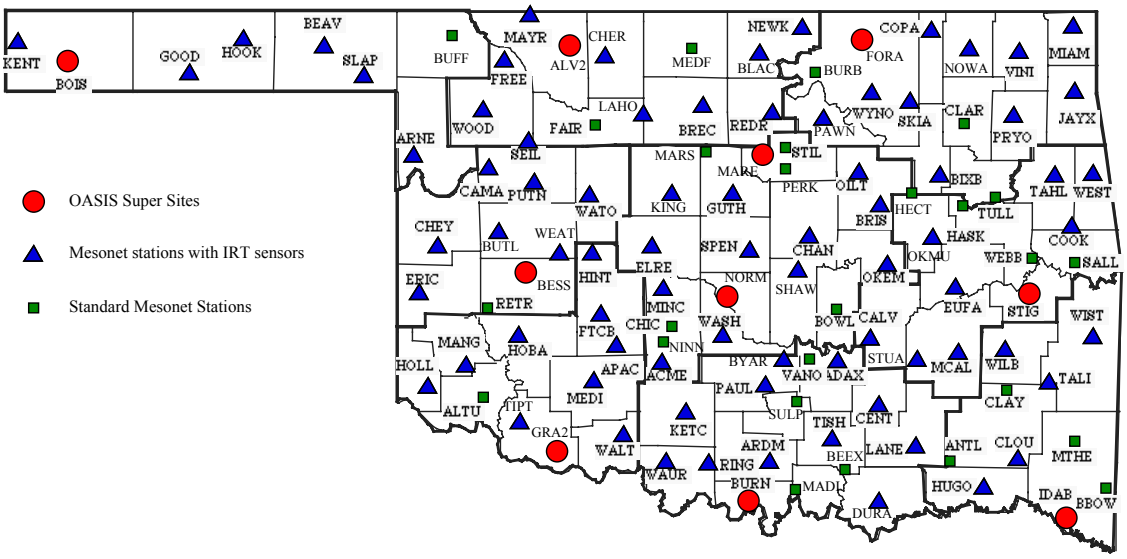

FIG. 1. Location of stations in the Oklahoma Mesonet.

where T_{sc} is the calibrated skin temperature (°C), T_{target} is the observed radiance temperature (°C), sb is the sensor body temperature (°C), and H_{sb}, K_{sb}, and P_{sb} are polynomials estimated as a function of the sensor body temperature as follows:

$$P_{sb} = 26.168 + 2.8291 * sb - 0.03329 * sb^2$$

$$H_{sb} = 5.8075 - 0.08016 * sb + 0.00849 * sb^2$$

$$K_{sb} = -85.943 + 11.740 * sb + 0.08477 * sb^2$$

2.2. *"Typical" data*

A diurnal cycle of air temperature (measured at 1.5 m) and T_{sc} on 11 May 2000 at Marena, Oklahoma is shown in Fig. 2. Downwelling solar radiation, as measured by a LiCor 200 pyranometer (Brock et al. 1995), also is shown. Both the air and skin temperatures cooled slightly near sunset at 0000 UTC (to convert to local standard time for Oklahoma, subtract 6 h) and then remained nearly steady overnight. The T_{sc} remained slightly cooler than the air temperature due to increased radiational cooling at the land surface. With sunrise at approximately 1200 UTC, both the air and skin temperature began a rapid increase. The T_{sc} increased quickly as a direct result of incoming solar radiation that heated the land surface. The time series shows that as downwelling solar radiation rapidly increased and decreased in response to intermittent cloudiness (specifically between 1600 and 1800 UTC), the T_{sc} also changed quickly. However, much smaller changes occurred in air temperature. This relationship illustrates the high sensitivity of T_{sc} to downwelling solar radiation.

T_{sc} remained warmer than air temperature for the majority of the daylight hours. While downwelling solar radiation peaked at solar noon (approximately 1800 UTC), the T_{sc} and air temperature peaked at about 1930 UTC and 2130 UTC, respectively. These lag times denote the fact that downwelling shortwave radiation

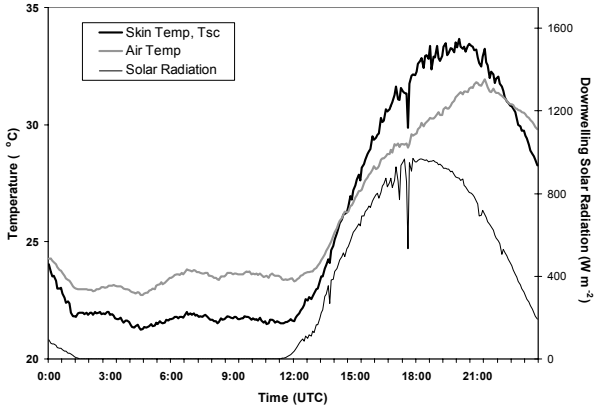

FIG. 2. Time series plot of the T_{sc} (°C), air temperature (°C), and downwelling solar radiation (W m^{-2}) at the Mesonet site near Marena, OK on 11 May 2000.

decreases in intensity after solar noon, but still exceeds upwelling shortwave and longwave radiation from the land surface for some time. This scenario yields an energy surplus for 2 to 4

hours after solar noon and substantially contributes to a lag between the time of maximum solar heating and the time of maximum air and skin temperatures (Ahrens 2000). Skin temperature, being somewhat more sensitive to the decrease in downwelling solar radiation, begins its decrease prior to the decrease in air temperature.

3. OPERATIONAL LIMITATIONS

3.1. Limitation of the calibration equation

Several significant problems result from using Eq. (1) with observed field data. First, the polynomials used in Eq. (1) appear to have been developed for a temperature range of only 5 to 35 °C. Thus, observations that fall outside of this temperature range may not be corrected properly by Eq. (1). Second, the correction equation was developed using a Celsius scale. When sensor body temperatures approach –8.42 °C, P_{sb} approaches zero; as P_{sb} nears zero, the second term in Eq. (1) approaches infinity. Consequently, for any low temperature estimate between -3 °C and –15 °C, Eq. (1) should not be used.

3.2. Cleaning problem

Mesonet personnel have found that the surface lens on the Apogee IRT sensor can be difficult to keep clean at remote sites. When dust, spider webs, or other debris cover the lens, the sensor is unable to sense the land-atmosphere interface as its target. Instead, the obstruction on the lens becomes the target. These instances are often easy to detect in the observed data because the target and sensor body temperatures remain nearly equal. Such instances can lead to errors in T_{sc} of greater than +/- 5 °C.

3.3. Footprint problem

Because the IRT sensor has a limited field of view (see Section 2.1), the observed T_{sc} values are sometimes not representative of larger scale surface features. Vegetation properties can be significantly different inside the 10 m x 10 m Mesonet site plot when compared to vegetation conditions surrounding the plot. Only native vegetation is found within the site area; crops and grazed land often surround the site. This limitation is easily seen across Oklahoma's winter wheat belt (a 150-km swath of winter wheat farms that stretch from southwest to north central Oklahoma; Haugland and Crawford 2002). Frequently during the summer (after the winter wheat harvest), a warm air temperature anomaly is apparent across the harvested winter wheat belt counties due to an increased partitioning of solar radiation to sensible heat flux. In contrast, the observed T_{sc} usually does not indicate the strong signal demonstrated by the air temperature. These contrasting results arise because the IRT sensor is located directly above the native vegetation within the site enclosure rather than the harvested wheat fields. In contrast, the air temperature sensor is impacted by a much larger upstream footprint which does include the harvested fields.

4. OBSERVATIONAL SPATIAL VARIABILITY

Interesting mesoscale features are revealed by investigating patterns of T_{sc} across Oklahoma during clear sky conditions. The observed T_{sc} values for 1500 UTC on 12 July 2000 are shown in Fig. 3a. A large area of low T_{sc} values extended across the Panhandle into northwest Oklahoma. This cool anomaly corresponded well with the portion of the state that received rainfall the night before (Fig. 3b). In fact, the *relatively* high T_{sc} values at the Goodwell (GOOD), Hooker (HOOK), and Slapout (SLAP) stations in the Panhandle is attributed to the lack of rainfall at those three sites. Dry conditions in those areas increased the partitioning of available energy to sensible heat flux and produced mesoscale warm anomalies across the Panhandle. At sites that did receive rainfall, the additional moisture prevented the land surface from warming as rapidly (due to increased latent heat flux).

The T_{sc} map (Fig. 3a) also revealed a lobe of warm values that extended from the Tipton (TIPT) and Grandfield (GRA2) stations in southwest Oklahoma northeast to the Kingfisher (KING) site. This area of warm T_{sc} resulted from an increase in downwelling solar radiation (Fig.3c). The incoming solar radiation heated the earth's surface, and with light winds (Fig.3d), was successful in increasing the T_{sc} in these areas. However, T_{sc} values do not reflect the numerous local maximas of solar radiation (Fig. 3c) throughout parts of eastern Oklahoma due to stronger wind speeds in those locations (Fig. 3d).

a)

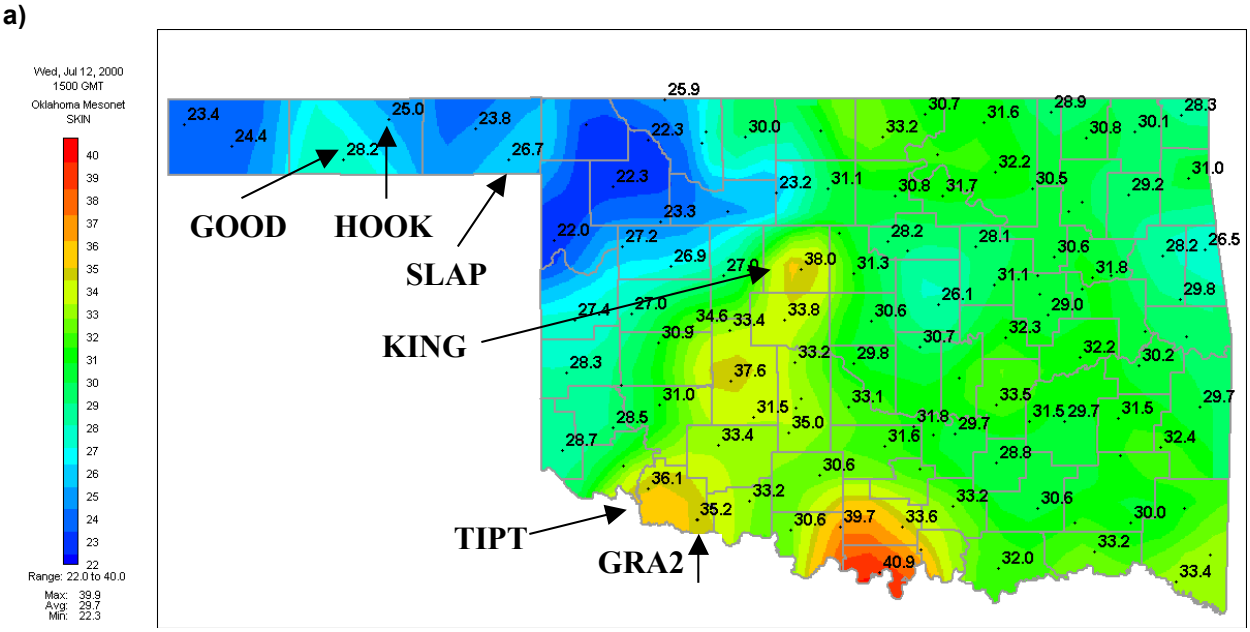
Wed, Jul 12, 2000
1500 GMT
Oklahoma Mesonet
SKIN
Range: 22.0 to 40.0
Max: 39.9
Avg: 29.7
Min: 22.3
GOOD
HOOK
SLAP
KING
TIPT
GRA2

b)

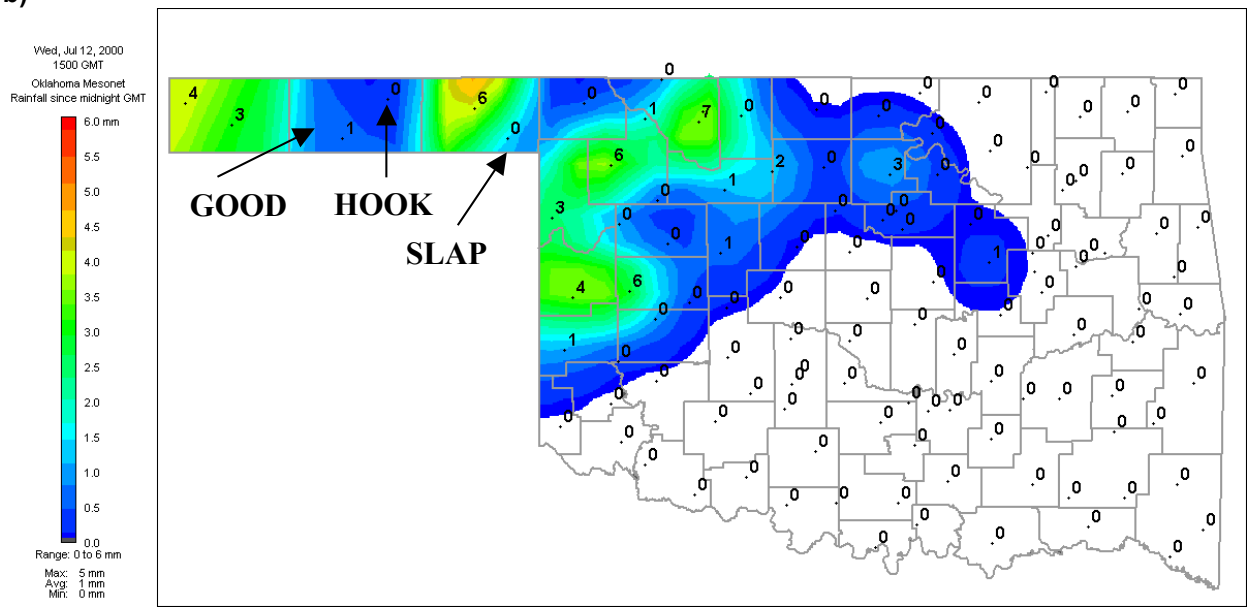
Wed, Jul 12, 2000
1500 GMT
Oklahoma Mesonet
Rainfall since midnight GMT
Range: 0 to 6 mm
Max: 5 mm
Avg: 1 mm
Min: 0 mm
GOOD
HOOK
SLAP

c)

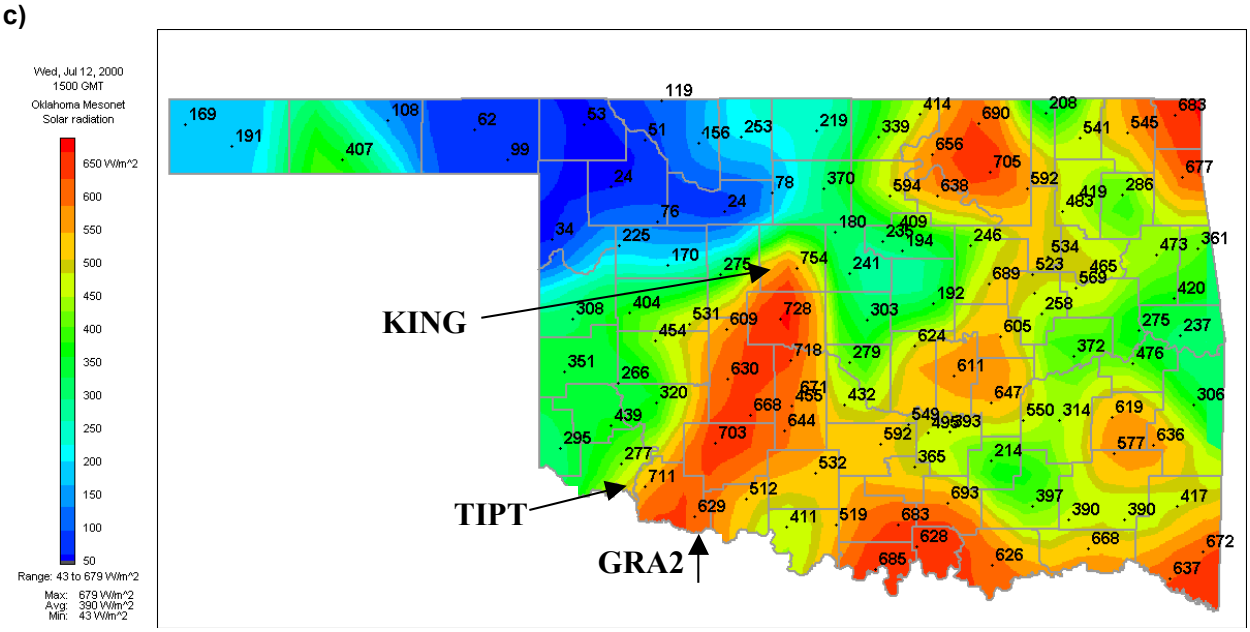

d)

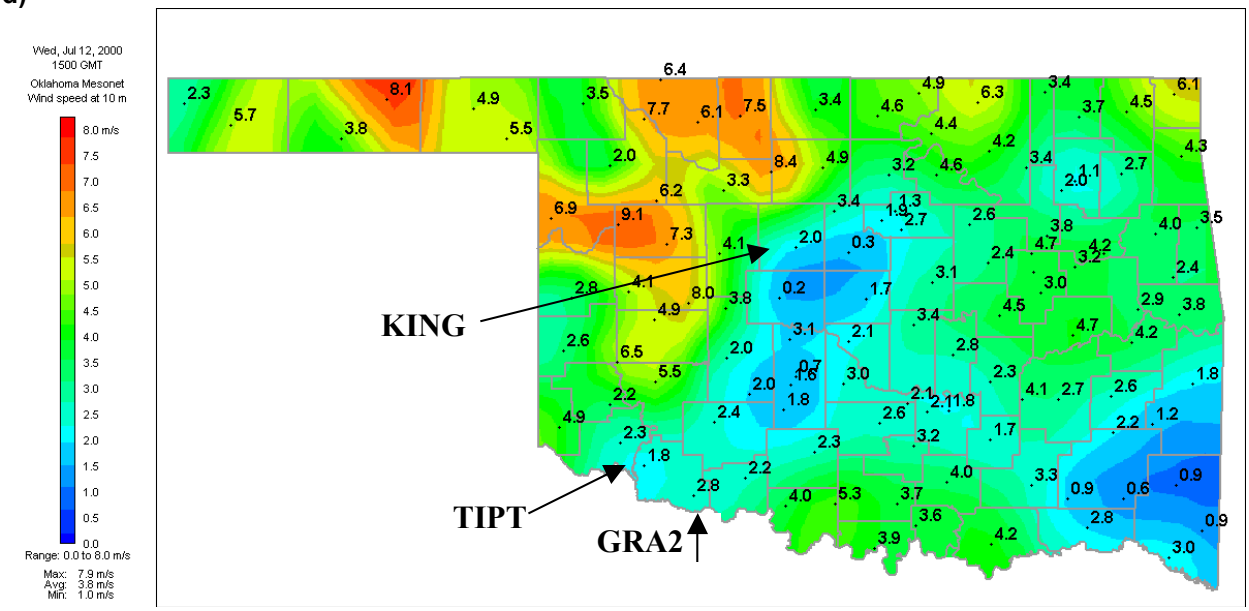

FIG. 3. (a) Mesonet station plot of the T_{sc} (°C) field across Oklahoma at 1500 UTC 12 July 2000. A large area of cool T_{sc} values is apparent across the Panhandle and northwest Oklahoma. (b) As in (a) except for accumulated rainfall (mm) since 0000 UTC. (c) As in (a) except for solar radiation (Wm^{-2}). (d) As in (a) except for wind speed (ms^{-1}).

5. SUMMARY

The Oklahoma Mesonet has installed IRT sensors at 89 sites across the state. Field evaluation of the sensors demonstrated several limitations related to continuous operational use outdoors. The calibration equation limits the use of the observations during the cold season. In addition, obstructions on the lens of a sensor can lead to erroneous observations. Lastly, care must be taken when extrapolating the observations spatially due to the sensor's narrow field of view.

Even with these limitations, the Oklahoma Mesonet's IRT network provides a unique opportunity to analyze long term, continuous, meso-scale observations of skin temperature across a large area. Such observations may prove critical in understanding many land-atmosphere interactions. Not only can the observations be used to estimate the partitioning of latent and sensible heat flux, they also provide beneficial "ground truth" estimates to validate remotely sensed estimates of skin temperature.

6. ACKNOWLEDGMENTS

The installation of the Oklahoma Mesonet's IRT network was made possible, in part by NSF Grant 125-5645 and EPSCoR 95 Grant NCC 5-171. Continued funding for maintenance of the network is provided by the taxpayers of the State of Oklahoma. The authors would like to thank Scott Richardson, James Kilby, David Grimsley, Leslie Cain, Kris Kesler, Ken Meyers, Bill Wyatt, and Thomas Smith for their professional assistance in maintaining the Oklahoma Mesonet. In addition, the authors would like to thank Ken Crawford, Director, and the staff of the Oklahoma Climatological Survey whose innovative work makes such projects possible.

7. REFERENCES

Ahrens, C. D., 2000: *Meteorology Today*. 6th ed. Brooks/Cole, 528 pp.

Brock, F. V., K. C. Crawford, R. L. Elliott, G. W. Cuperus, S. J. Stadler, H. L. Johnson, and M. D. Eilts, 1995: The Oklahoma Mesonet: A technical overview, *J. Atmos. Oceanic Technol.*, **12**, 5-19.

Brotzge, J. A., S. J. Richardson, K. C. Crawford, T. W. Horst, F. V. Brock, K. S. Humes, Z. Sorbjan, and R. L. Elliott, 1999: The Oklahoma Atmospheric Surface-layer Instrumentation System (OASIS) Project. Preprints, *13th Conf. on Bound.-Lay. Turb.*, Dallas, TX, Amer. Meteor. Soc., 612-615.

Bugbee, B., M. Droter, O. Monje, and B. Tanner, 1998: Evaluation and modification of commercial infra-red transducers for leaf temperature measurement. *Adv. Space Res.*, **22**, 1425-1434.

Cahill, A. T., M. B. Parlange, and J. D. Albertson, 1997: On the Brutsaert temperature roughness length model for sensible heat flux estimation. *Water Resour. Res.,* **33**, 2315-2324.

Crago, R. D., 1998: Radiometric and equivalant isothermal surface temperatures. *Water Resour. Res.,* **34**, 3017-3023.

English, S. J., 1999: Estimation of temperature and humidity profile information from microwave radiances over different surface types. *J. Appl. Meteorol.*, **38**, 1526-1541.

Haugland, M. J., and K. C. Crawford, 2002: The diurnal cycle of dewpoint across Oklahoma's winter wheat belt. Preprints, 13*th Symp. On Global Change and Climate Variations*, Orlando, FL, Amer. Meteor. Soc., 254-256.

Ibanez, M., P. J. Perez, J. I. Rosell, and F. Castellvi, 1999: Estimation of the latent heat flux over full canopy covers from the radiative temperature. *J. Appl. Meteor.*, **38**, 423-431.

Katul, G. G., and M. B. Parlange, 1992: Estimation of bare soil evaporation using skin temperature measurements. *J. Hydrol.*, **132**, 91-106.

Kustas, W. P., B. J. Choudhury, M. S. Moran, R. J. Reginato, R. D. Jackson, I. W. Gray, and H. L. Weaver, 1989: Determination of sensible heat flux using thermal infrared data. *Agric. For. Meteor.*, **44**, 197-216.

Lhomme, J. P., A. Chehbouni, and B. Monteny, 2000: Sensible heat flux-rariometric surface temperature relationship over sparse vegetation: Parameterizing B^{-1}. *Bound.-Layer Meteor.*, **97**, 431-457.

Monin, A. S., and A. M. Obukhov, 1954: Basic laws of turbulent mixing in the ground layer of the atmosphere. *Tr. Geofiz. Alad. Nauk. SSSR*, **24**, 163-187.

Sugita, M., and W. Brutsaert, 1996: Optimal measurement strategy for surface temperature to determine sensible heat flux from an isothermal vegetation. *Water Resour. Res.,* **32**, 2129-2134.

Voogt, J. A. and C. S. B. Grimmond, 2000: Modeling surface sensible heat flux using surface radiative temperatures in a simple urban area. *J. Appl. Meteor.*, **39**, 1679-1699.